Chapter 7
Extended Structure of Rat Islet Amyloid Polypeptide in Solution

Lei Wei, Ping Jiang, Malathy Sony Subramanian Manimekalai, Cornelia Hunke, Gerhard Grüber, Konstantin Pervushin and Yuguang Mu

Abstract The process of islet amyloid polypeptide (IAPP) formation and the prefibrillar oligomers are supposed to be one of the pathogenic agents causing pancreatic β-cell dysfunction. The human IAPP (hIAPP) aggregates easily and therefore, it is difficult to characterize its structural features by standard biophysical tools. The rat version of IAPP (rIAPP) that differs by six amino acids when compared with hIAPP, is not prone to aggregation and does not form amyloid fibrils. Similar to hIAPP it also demonstrates random-coiled nature in solution. The structural propensity of rIAPP has been studied as a hIAPP mimic in recent works. However, the overall shape of it in solution still remains elusive. Using small angle X-ray scattering (SAXS) measurements combined with nuclear magnetic resonance (NMR) and molecular dynamics simulations (MD) the solution structure of rIAPP was studied. An unambiguously extended structural model with a radius of gyration of 1.83 nm was determined from SAXS data. Consistent with previous studies, an overall random-coiled feature with residual helical propensity in the N-terminus was confirmed. Combined efforts are necessary to unambiguously resolve the structural features of intrinsic disordered proteins.

Keywords IAPP · NMR · Molecular dynamics simulations

7.1 Introduction

Islet amyloid polypeptide (IAPP) is a peptide hormone secreted by the endocrine β-cells of the pancreas together with insulin [1]. It has 37 amino acids with a disulfide bond between residue 2 and 7 in the N-terminus. In solution, IAPP is characterized as a natively disordered protein [2–6]. In patients with type 2

L. Wei · P. Jiang · M.S.S. Manimekalai · C. Hunke · G. Grüber · K. Pervushin · Y. Mu (✉)
School of Biological Sciences, Nanyang Technological University, 60 Nanyang Drive, Singapore, Singapore
e-mail: ygmu@ntu.edu.sg

D. Wei et al. (eds.), *Advance in Structural Bioinformatics*, Advances in Experimental Medicine and Biology 827, DOI 10.1007/978-94-017-9245-5_7

diabetes, IAPP changes its conformation to form amyloid fibers [7]. The process of IAPP amyloid formation and the prefibrillar oligomers are supposed to be one of the pathogenic agencies causing pancreatic β-cell dysfunction [8–11]. Thus the structural characterization of IAPP in the form of monomer or small oligomer states would be beneficial towards the full understanding of the toxicity mechanism of IAPP oligomers.

The human IAPP (hIAPP) aggregates easily and therefore, it is difficult to characterize its structural features by standard biophysical tools. Whereas the rat version of IAPP (rIAPP), that differ by six amino acids compared with hIAPP, is not prone to aggregation and does not form amyloid fibrils. But similar to hIAPP it also demonstrates random-coiled nature in solution. The structural propensity of rIAPP has been studied as a hIAPP mimic in several of the recent works [2–5, 12, 13]. However, the overall shape of it in solution still remains elusive. Here, we focus on resolving the low resolution structure of this peptide in solution by small angle X-ray scattering (SAXS) measurements and with complementary nuclear magnetic resonance (NMR) data. Further, these structural information were utilized to assess the ability of the three commonly used classic energy functions (force fields) for simulating the intrinsic disordered peptides/proteins.

7.2 Materials and Methods

7.2.1 Systems and NMR Spectroscopy

The ^{15}N uniformly labeled rIAPP sample preparation and NMR experiments have been described in details in our last publication [3]. Briefly, ^{15}N-HSQC, ^{15}N-TOCSY-HSQC (τmix = 120 ms) and ^{15}N-NOESY-HSQC (τmix = 200 ms) were performed using a Bruker Advance II 700 MHz spectrometer at 25 °C. The data were collected on a sample containing 50 μM ^{15}N uniformly labeled rIAPP (in 5 mM potassium phosphate buffer, 10 mM KCl, 3 % D_2O, pH 6). The spectra were analyzed and the chemical shifts were assigned with CARA software (www.nmr.ch). Peaks were picked manually from the 3D ^{15}N-NOESY-HSQC spectrum. The peak list, together with the chemical shift assignments were used as the input for structure calculations by CYANA 2.0 [14].

7.2.2 Small Angle X-ray Scattering Experiments

The synchrotron radiation X-ray scattering data for rIAPP were collected following standard procedures on the X33 SAXS camera of the EMBL Hamburg located on a bending magnet (sector D) on the storage ring DORIS III of the Deutsches Elektronen Synchrotron (DESY).

7.2.3 Molecular Dynamics Simulations

Classic molecular dynamics simulations were performed on rIAPP using three different force fields, AMBER03 [15] with recent modifications [16], OPLSAA [17] and CHARMM with CMAP [18, 19]. All simulations lasted 50 ns, which began with the NMR model 1 that has a Rg value of 1.78 nm. A dodecahedron box of size 7 nm was used with 7,869 water molecules (SPC model) and four chloride ions. The simulation was performed using Gromacs simulation package [20], during which all bonds involving hydrogen atoms were constrained in length according to LINCS protocol [21] with the integration step 2 fs. Non-bonded pair lists were updated every five integration steps. The protein and the water were separately coupled to the external heat bath with the relaxation time of 0.1 ps. The structure snapshots were output every 1 ps. Electrostatic interactions were treated with the particle mesh Ewald method [22] with a cutoff of 0.9 nm, while for the van der Waals interactions a cutoff of 1.4 nm was used. The simulations were repeated three times for each force field with different initial velocities. The helical structures of peptides were assessed by DSSP algorithm [23].

7.3 Results

7.3.1 Solution Structure Obtained from SAXS Measurements

Solution X-ray scattering experiments have been performed with the aim to determine the low resolution structure of rIAPP in solution. SAXS patterns from solutions of the peptide were recorded as described in "Materials and Methods" to yield the final composite scattering curve in Fig. 7.1a, showing that the peptide is monodispersed in the solution. Inspection of the Guinier plots at low angles indicated good data quality and no protein aggregation. The radius of gyration R_g of rIAPP is 1.83 ± 0.1 nm and the maximum dimension D_{max} of the peptide is 6.4 ± 0.4 nm (Fig. 7.1b). The solution shape of rIAPP was restored ab initio from the scattering pattern in Fig. 7.1a using the dummy residues modeling program DAMMIN [24], which fitted well to the experimental data in the entire scattering range (a typical fit displayed in Fig. 7.1a, red curve, has the discrepancy of $\chi^2 = 1.061$). Ten independent reconstructions yielded reproducible models and the average model is displayed in Fig. 7.2. rIAPP appears as an elongated molecule with a length of 6.4 nm and an overall spiral-like shape.

The solution structure of rIAPP has also been studied by us through NMR spectroscopy in our previous work [3]. Although the residual helical structure was relatively well-defined, the global structures generated by applying NMR constraints were quite heterogeneous, which was due to the lack of long-range constraints. Twenty structural models generated from NMR constrains are shown in Fig. 7.3. The radius of gyration (R_g) for this structure ensemble ranges from 1.1 to 1.78 nm.

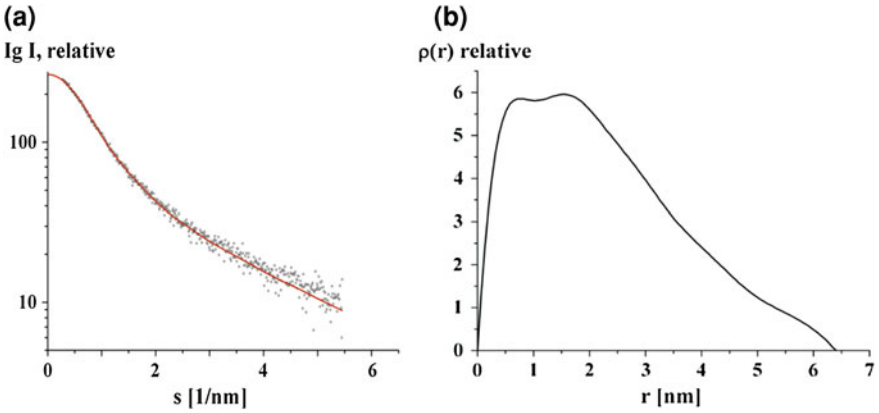

Fig. 7.1 Small-angle X-ray scattering data of rIAPP. **a** Experimental scattering data (*circle*) and the *fitting curves* (*line*; *green* experimental, *red* calculated from ab initio model) for rIAPP. **b** The distance distribution function of the same peptide

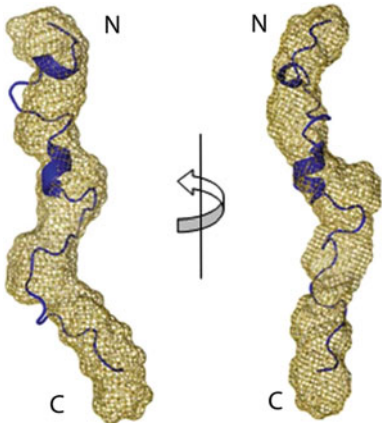

Fig. 7.2 Superposition of the DAMMIN model of rIAPP (*mashed shape*) with the NMR solution structure (*blue*) of the same peptide. The two models are rotated clockwise by around 90° along the Y-axis. The two helical regions are residue 9–12 and residue 15–17

Out of the 20 structural models we do found one model (NMR1) with an R_g of 1.78 nm. This NMR1 model and the solution shape, determined by SAXS ($R_g = 1.83$ nm), were superimposed with the program SUBCOMP [25] which showed good fitting with an r.m.s. deviation of 1.47 Å (Fig. 7.2). When we repeated the structural refinement processes using NMR constrains, only 5 % of the generated structural models have R_g larger than 1.73 nm. Clearly combing local structural information from NMR measurement with the global structural profile from SAXS can greatly narrow down the configuration space of the model structures. Thus the

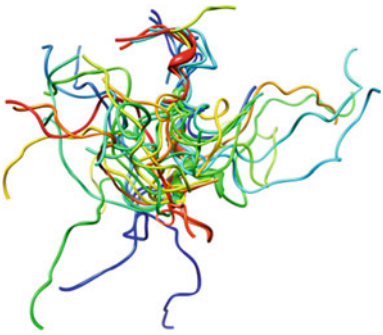

Fig. 7.3 The superimposing of 20 structure models from NMR constraints. The average helical residue number is 5.75

SAXS refined structural models of rIAPP are quite extended. Previously the dynamics of contact formation between the N- and C-termini in monomeric IAPP from human and rat were probed by triplet quenching technique [5]. This showed that the relaxation rates are approximately 2-fold faster for hIAPP than for rIAPP, which indicated that rIAPP is always more expanded than hIAPP.

7.3.2 Evaluation of Three Force Fields

Three all-atom force fields, AMBER03d [16], CHARMM [18] and OPLSAA [17], were employed to simulate this peptide in the presence of explicit water. The initial structure was taken from the elongated NMR1 model (Fig. 7.2 and 7.4a). The back-calculated scattering curve from the NMR1 model with CRYSOL program [26] gave a χ^2 value of 2.93 after superimposition onto the experimental data (Fig. 7.4c, solid line), indicating the consistency with both the experimental NMR- and SAXS data. Unfortunately, the configuration of the solution model cannot be maintained within the three force fields. In the AMBER03d and OPLSAA force field simulations the peptide collapses quickly in the first 10 ns from the initial R_g value of 1.78–1.1 nm (Fig. 7.5a). These compact conformations (Fig. 7.5b) were nearly unchanged during the following 40 ns simulations. The back-calculated scattering curve from such compact model (Fig. 7.5b) with CRYSOL resulted in a χ^2 value of 7.49 after superimposition with the experimental data (Fig. 7.4c, blue dashed line).

This compact feature of rIAPP has also been proposed from theoretical simulations and infrared spectroscopy data [4]. However, a compact model is not consistent with the experimental SAXS- and NMR data presented. The simulated conformations using CHARMM force field have larger R_g values, than the other two force fields (Fig. 7.5a), however, they are highly helical (Fig. 7.5b). The average number of helical residues is above 19 (more than half of the residues of the peptide) during the 50 ns trajectory. Such highly helical propensity is in contradiction with the overall random-coil nature of the peptide resolved by NMR

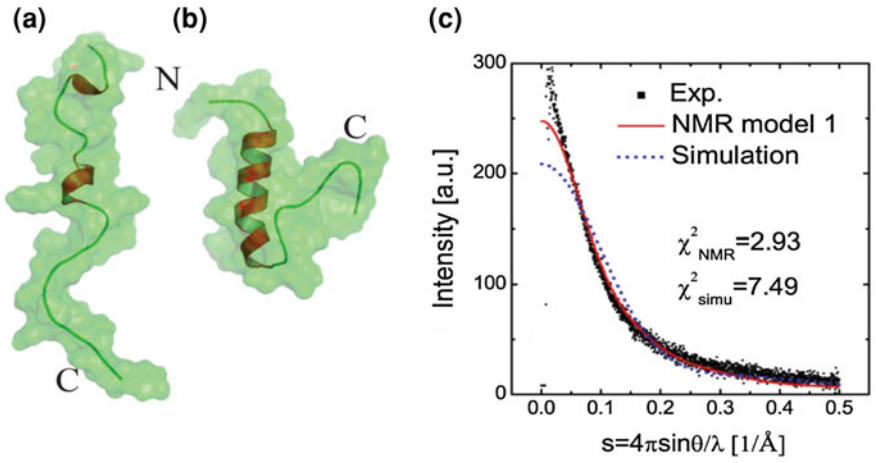

Fig. 7.4 Comparison of NMR1 model (**a**) and simulation model of AMBER03d (**b**) scattering intensities between experimental data and calculated from structural models (**c**)

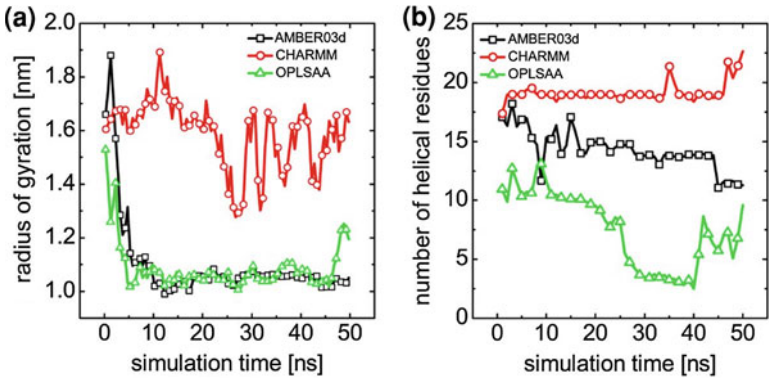

Fig. 7.5 Evolution of radius of gyration, Rg, **a** and the number of backbone hydrogen bonds **b** of rat IAPP from three different force fields simulations. Each data point is an averaged value during 1 ns simulation

measurement [2, 3]. The average helical residue number of 20 NMR structural models (Fig. 7.3) is only 5.75. Two more simulations in each type of force fields have been performed with different initial velocities in which similar results were obtained.

7.4 Conclusions

In summary we combined NMR measurements, which mainly provided local secondary structure information in this case, and SAXS data, which delivered a global structural profile, to resolve an extended, random-coiled structural model for the rat IAPP peptide. The presented structure will provide an invaluable reference to further study the conformational propensity of more disease related hIAPP.

References

1. Jaikaran E, Clark A (2001) Islet amyloid and type 2 diabetes: from molecular misfolding to islet pathophysiology. Biochim Biophys Acta-Mol Basis Dis 1537:179–203
2. Williamson JA, Miranker AD (2007) Direct detection of transient alpha-helical states in islet amyloid polypeptide. Protein Sci 16:110–117
3. Wei L, Jiang P, Yau YH, Summer H, Shochat SG, Mu Y, Pervushin K (2009) Residual structure in islet amyloid polypeptide mediates its interactions with soluble insulin. Biochemistry 48:2368–2376
4. Reddy AS, Wang L, Lin YS, Ling Y, Chopra M, Zanni MT, Skinner JL, De Pablo JJ (2010) Solution structures of rat amylin peptide: simulation, theory, and experiment. Biophys J 98:443–451
5. Vaiana SM, Best RB, Yau WM, Eaton WA, Hofrichter J (2009) Evidence for a partially structured state of the amylin monomer. Biophys J 97:2948–2957
6. Dupuis NF, Wu C, Shea JE, Bowers MT (2009) Human islet amyloid polypeptide monomers form ordered beta-hairpins: a possible direct amyloidogenic precursor. J Am Chem Soc 131:18283–18292
7. Haataja L, Gurlo T, Huang CJ, Butler PC (2008) Islet amyloid in type 2 diabetes, and the toxic oligomer hypothesis. Endocr Rev 29:303–316
8. Campioni S, Mannini B, Zampagni M, Pensalfini A, Parrini C, Evangelisti E, Relini A, Stefani M, Dobson CM, Cecchi C, Chiti F (2010) A causative link between the structure of aberrant protein oligomers and their toxicity. Nat Chem Biol 6:140–147
9. Hull RL, Westermark GT, Westermark P, Kahn SE (2004) Islet amyloid: a critical entity in the pathogenesis of type 2 diabetes. J Clin Endocrinol Metab 89:3629–3643
10. Gurlo T, Ryazantsev S, Huang CJ, Yeh MW, Reber HA, Hines OJ, O'Brien TD, Glabe CG, Butler PC (2010) Evidence for proteotoxicity in beta cells in type 2 diabetes toxic islet amyloid polypeptide oligomers form intracellularly in the secretory pathway. Am J Pathol 176:861–869
11. Janson J, Ashley RH, Harrison D, McIntyre S, Butler PC (1999) The mechanism of islet amyloid polypeptide toxicity is membrane disruption by intermediate-sized toxic amyloid particles. Diabetes 48:491–498
12. Soong R, Brender JR, Macdonald PM, Ramamoorthy A (2009) Association of highly compact type 2 diabetes related islet amyloid polypeptide intermediate species at physiological temperature revealed by diffusion nmr spectroscopy. J Am Chem Soc 131:7079–7085
13. Nanga RPR, Brender JR, Xu JD, Hartman K, Subramanian V, Ramamoorthy A (2009) Three-dimensional structure and orientation of rat islet amyloid polypeptide protein in a membrane environment by solution nmr spectroscopy. J Am Chem Soc 131:8252–8261

14. Güntert P (2003) Automated NMR protein structure calculation. Prog Nucl Magn Reson Spectrosc 43:105–125
15. Duan Y, Wu C, Chowdhury S, Lee MC, Xiong GM, Zhang W, Yang R, Cieplak P, Luo R, Lee T, Caldwell J, Wang JM, Kollman P (2003) A point-charge force field for molecular mechanics simulations of proteins based on condensed-phase quantum mechanical calculations. J Comput Chem 24:1999–2012
16. Best RB, Hummer G (2009) Optimized molecular dynamics force fields applied to the helix-coil transition of polypeptides. J Phys Chem B 113:9004–9015
17. Kaminski GA, Friesner RA, Tirado-Rives J, Jorgensen WL (2001) Evaluation and reparametrization of the OPLS-AA force field for proteins via comparison with accurate quantum chemical calculations on peptides. J Phys Chem B 105:6474–6487
18. Mackerell AD, Feig M, Brooks CL (2004) Extending the treatment of backbone energetics in protein force fields: limitations of gas-phase quantum mechanics in reproducing protein conformational distributions in molecular dynamics simulations. J Comput Chem 25:1400–1415
19. Bjelkmar P, Larsson P, Cuendet MA, Hess B, Lindahl E (2010) Implementation of the CHARMM force field in GROMACS: analysis of protein stability effects from correction maps, virtual interaction sites, and water models. J Chem Theory Comput 6:459–466
20. David Van Der Spoel EL, Hess B, Groenhof G, Mark AE, Berendsen HJC (2005) GROMACS: fast flexible and free. J Comput Chem 26:1701–1718
21. Hess B, Bekker H, Berendsen HJC, Fraaije J (1997) LINCS: a linear constraint solver for molecular simulations. J Comput Chem 18:1463–1472
22. Darden T, York D, Pedersen L (1993) Particle mesh Ewald: an N•log(N) method for Ewald sums in large systems. J Chem Phys 98:10089–10092
23. Kabsch W, Sander C (1983) Dictionary of protein secondary structure: pattern recognition of hydrogen-bonded and geometrical features. Biopolymers 22:2577–2637
24. Svergun DI (1999) Restoring low resolution structure of biological macromolecules from solution scattering using simulated annealing. Biophys J 76:2879–2886
25. Kozin MB, Svergun DI (2001) Automated matching of high- and low-resolution structural models. J Appl Crystallogr 34:33–41
26. Svergun D, Barberato C, Koch MHJ (1995) CRYSOL—a program to evaluate X-ray solution scattering of biological macromolecules from atomic coordinates. J Appl Crystallogr 28:768–773